Polymer Chemistry

REVIEW

View Article Online
View Journal | View Issue

Cite this: *Polym. Chem.*, 2020, **11**, 166

Tuning chromatic response, sensitivity, and specificity of polydiacetylene-based sensors

Max Weston, Angie Davina Tjandra and Rona Chandrawati *

Polydiacetylenes (PDAs) are a class of conjugated polymers with unique optical properties that make them excellent materials for the construction of colorimetric sensors. Self-assembly of amphiphilic diacetylene monomers in solution and photopolymerization of neighboring diacetylene groups yield blue-phase PDAs. PDAs can be functionalized with a wide range of recognition elements, and chemical and biological recognition events, *e.g.* protein-antibody interaction, nucleic acid hybridization, pH change, can generate a visible blue-to-red chromatic transition of PDA. The color change mechanism remains to be fully elucidated and is analyte dependent, and its understanding is key to optimizing PDA-based sensing systems. In this review, we provide an overview of different methods of tuning the chromatic response, sensitivity, and specificity of PDA-based sensors. It draws conclusions regarding the relationship between these variables, specifically sensitivity and specificity, to guide the future development of PDA sensing systems.

Received 28th June 2019,
Accepted 18th August 2019

DOI: 10.1039/c9py00949c

rsc.li/polymers

Introduction

Polydiacetylenes (PDAs) are a class of conjugated polymers with interesting optical features that make them attractive building blocks for colorimetric sensors. Amphiphilic diacetylene (DA) monomers self-assemble into a range of supramolecular structures in aqueous solution. In organized structures that exhibit favorable geometric arrangement and packing orientation, neighboring DA monomers undergo topochemical polymerization when exposed to 254 nm UV light *via* a 1,4-addition reaction to form alternating ene–yne polymer chains.[1–4] The conjugated product has a delocalized network of π electrons that instill PDA with its unique optical properties. Polymerization typically yields blue-phase PDAs with a characteristic absorption peak at ~640 nm, which can be monitored by UV-Vis spectrophotometry. Stimulus such as heat, pH, pressure, chemical and biological recognition events can induce a blue-to-red color transition of PDA, which can be easily detected by the naked eye (Fig. 1). Red-phase PDAs have an absorption peak at ~540 nm. The change in absorption peak and color is due to a shift in the energy required to shift π electrons from HOMO to LUMO molecular orbital. The color change mechanism is complex and is not entirely understood.

School of Chemical Engineering and Australian Centre for Nanomedicine (ACN), The University of New South Wales (UNSW Sydney), Sydney, NSW 2052, Australia. E-mail: rona.chandrawati@unsw.edu.au

Max Weston

Max Weston received his Bachelor of Chemical and Biomolecular Engineering from The University of Sydney in 2016. He is now a PhD student under the supervision of Dr Rona Chandrawati at The University of New South Wales (UNSW Sydney), Australia. His research focuses on developing polydiacetylene-based biosensors for the detection of food contaminants and disease biomarkers.

Angie Davina Tjandra

Angie Davina Tjandra obtained her Bachelor of Engineering in Chemical and Biomolecular Engineering from The University of Sydney in 2018. She is currently a research assistant working under the supervision of Dr Rona Chandrawati at The University of New South Wales (UNSW Sydney), Australia. Her research focuses on developing bioinspired nanomaterials for early stage disease detection.

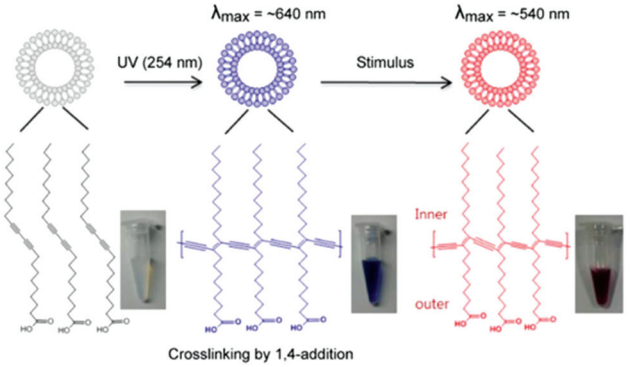

Fig. 1 Chemical structure of polydiacetylene and its chromatic properties. Polymerized backbone of vesicles and blue-to-red color transition is shown. Adapted from ref. 23 with permission from MDPI, copyright [2012].

However, the blue to red transition is usually attributed to a conformational or twisting effect on the polymer backbone that changes the effective conjugation length. PDAs can be functionalized with a wide range of recognition elements (*e.g.* antibody, peptide, and nucleic acid) *via* covalent conjugation or insertion into the bilayer of PDA vesicles for the detection of an array of analytes, including bacteria,[5–7] viruses,[8,9] proteins,[10–12] antibiotics,[13,14] surfactants,[15,16] metal ions,[17,18] and volatile organic compounds.[19–22] The color change is triggered by a perturbation in the conjugated backbone of PDA, which leads to a change in effective conjugation length. The mechanism remains to be fully elucidated, however its understanding is thought to be a key to optimizing PDA-based sensing systems.

A substantial body of academic research has been developed since the first study on PDA was conducted by Wegner in 1969.[24] In his initial studies, he photopolymerized 1,6-bis-hydroxy hexa-2,4-diyne to create purple crystals that then transitioned into red-phase PDA. Several excellent reviews exist that document and discuss work related to PDA sensors since they were first conceived. In 2012, Chen *et al.* reviewed different methods of PDA functionalization including covalent bonding and insertion of receptor molecules into the hydrophobic moiety of vesicles.[25] Jelinek and Ritenberg discussed the different pathways to PDA synthesis and PDA applications.[26] More recently, Wen *et al.* reviewed a wide range of synthesis techniques, characterization methods, and applications of PDA in drug delivery and tissue engineering.[27] Lebègue *et al.* have completed a more specific review on the application of PDAs in the detection of microorganisms.[7] Qian and Städler reviewed the most recent PDA developments in relation to their structural features.[28]

The application of PDA to sense an array of analytes and environmental stimuli highlights its versatility as a sensing platform. However, it does draw concerns relating to sensor specificity, which is a necessary attribute for out of lab applications. Chemical and biological detection can be achieved with excellent specificity by appropriate design of the sensor's recognition element. However, common methods used to improve sensor detection limits also create an undesired increase in chromatic sensitivity to light, heat, and the chemical environment. To achieve widespread and commercial application of PDA sensors, methods of tuning sensitivity that can maximize sensitivity towards the desired analyte while minimizing sensitivity towards environmental stimulus are required. The intention of this review is to provide insights into different methods of tuning PDA sensitivity and how this relates to other sensing properties, particularly specificity. Depending on its intended application, whether for thermal, mechanical, biological or chemical target sensing, the importance of the chromic transition detection limit, stability and reversibility vary. For example, while the chromic reversibility of PDA system is generally crucial for thermo-sensing applications, such an attribute is usually not desired for analyte detection as it is susceptible to a false-negative remark. Herein, six techniques for controlling PDA sensitivity are reviewed. The conclusion of this review will serve as a guide for future research that intends to optimize PDA in the context of its desired application to facilitate the translation from academic curiosity into fully realized technology.

Rona Chandrawati

Dr Rona Chandrawati obtained her PhD from the Department of Chemical and Biomolecular Engineering at The University of Melbourne in 2012. She was then a Marie Curie Fellow at Imperial College London prior to joining The University of Sydney as a Lecturer in 2015. In 2018, she joined The University of New South Wales (UNSW Sydney), Australia as a Senior Lecturer, Scientia Fellow, and Australian Research Council DECRA Fellow. Her research interests include bionanomaterials for drug delivery and chemical and biological sensing.

Photopolymerization time

PDA systems are formed during the photopolymerization of self-assembling DA monomers. On a molecular scale, the photopolymerization process induces molecular displacement and a change in bond angle which initiates the development of internal chemical strain within the PDA assemblies, forming a thermodynamically metastable system.[29] As the extent of the internal chemical strain increases with the topochemical polymerization, the unique PDA chromatic properties could subsequently be tuned by controlling the UV irradiation time.

Colorimetric response (CR) is a standard method for quantifying blue-to-red color transition of PDA, developed by

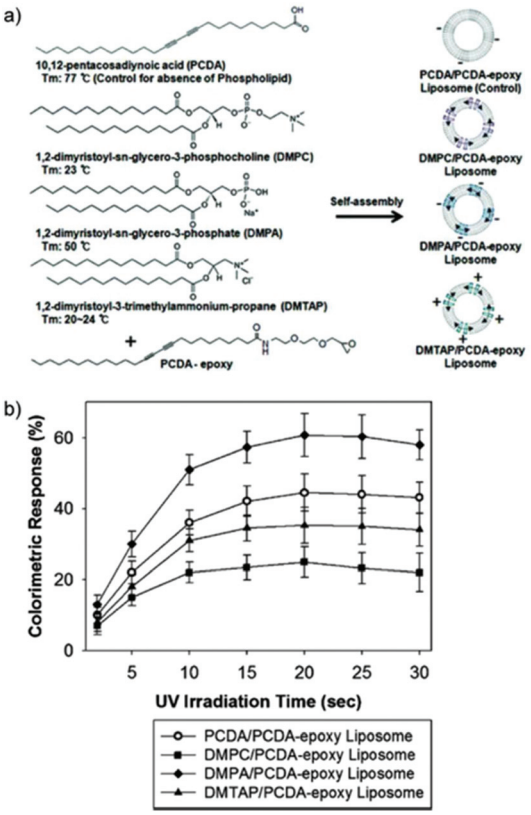

Fig. 2 (a) Different kinds of PDA-phospholipid liposomes. (b) Colorimetric response (CR) of various PDA-phospholipid liposomes at different 254 nm UV irradiation time periods. Thermochromic CR was measured after heat treatment of the liposomes at 70 °C for 3 min in the oven. Reproduced from ref. 31 with permission from the American Chemical Society, copyright [2012].

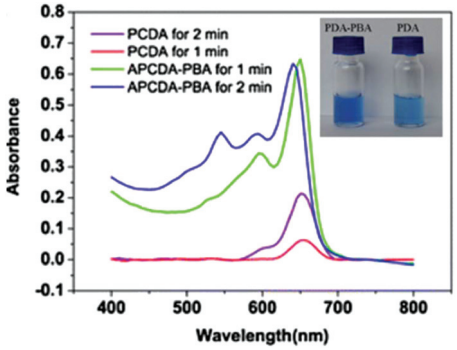

Fig. 3 UV-Vis absorption spectra of PDA and PDA-PBA vesicles irradiated with UV for 1 or 2 min. Inset: Photograph of PDA-PBA solution (1 min irradiation) and PDA solution (2 min irradiation). A stronger blue color was obtained in response to a greater extent of polymerization. Reproduced from ref. 32 with permission from Springer Nature, copyright [2016].

Charych and coworkers.[30] Kang *et al.* reported the enhanced CR of several PDA-phospholipid thermosensor liposomes with longer UV (254 nm 1 mW cm^{-2}) irradiation time (Fig. 2).[31] The colorimetric transition was monitored using a UV-Vis spectrometer after 70 °C heating in the oven for 3 min. The increased CR with longer irradiation time was due to the greater degree of DA monomer conversion into PDAs. Fig. 2 also shows that regardless of the lipid composition inserted into PDA liposomes, a consistent trend at which the CR plateau after 20 seconds of irradiation indicated that the PDA-phospholipid composites have reached their saturation point.

A similar saturation effect was observed in the chemosensor developed by Jia *et al.*[32] The authors compared the effects of UV (254 nm) irradiation time on the polymerization of pure PDA and PDA functionalized with phenylboronic acid (PDA-PBA) for the detection of hydrogen peroxide (H_2O_2). Both sensors were placed within a 30 cm distance to the UV source during the polymerization process. The absorbance spectra of PDA-PBA irradiated for 1 and 2 min showed no significant difference in the A_{650} peak, which means that 1 min was sufficient to fully saturate the PDA-PBA vesicles (Fig. 3). On the other hand, the absorption of pristine PDA at 650 nm increased significantly when the irradiation time was increased from 1 min to 2 min, indicating longer irradiation time resulted in a greater extent of PDA polymerization. The addition of PBA was reported to ease the photopolymerization process due to the presence of B–O and C–H bonds.

Traiphol *et al.* extensively studied the effect of photopolymerization time on the color transition temperature of thermoreversible PDA/ZnO nanocomposites.[29] PDA was prepared from the commonly used 10,12-pentacosadynoic acid (PCDA) and irradiated under 254 nm, 10 W UV light with a fixed distance of 5 cm. The irradiation time was varied from 10 seconds up to 120 min. Photographs of the composites in response to temperature change were recorded as the sample was heated from 30° to 95 °C to determine the effect of photoirradiation time on chromic transition temperature, and after it was cooled back to 30 °C to observe its thermochromic reversibility. Fig. 4a shows the color transition of PDA/ZnO composites observable by the naked eye in response to temperature variation at different photopolymerization time. It was found that longer photopolymerization time decreases the color transition temperature of the PDA/ZnO composites due to the increase in PDA chain length, which in turn causes the rearrangement of the conjugated backbone. Longer photopolymerization also enables higher degree of melting of the corresponding DA monomers, thus enhancing the PDA color intensity.[6,33]

The opposite trend was observed on the chromic reversibility. Prolonged UV irradiation only partially reversed the color transition, as evidenced by the purplish-blue shade of the cooled samples (Fig. 4a, 90 min and 120 min composites). After 5 min irradiation, the PDA chain began to form a new electronic species with λ_{max} shifted from about 640 nm to 690 nm, and later absorbance at 690 nm gradually decreased with a new blue-shift peak observed at 612 nm (Fig. 4b). Longer photopolymerization time results in a higher magnitude of change of strain within the conjugated ene–yne backbone. This prohibits segmental relaxation back to its original

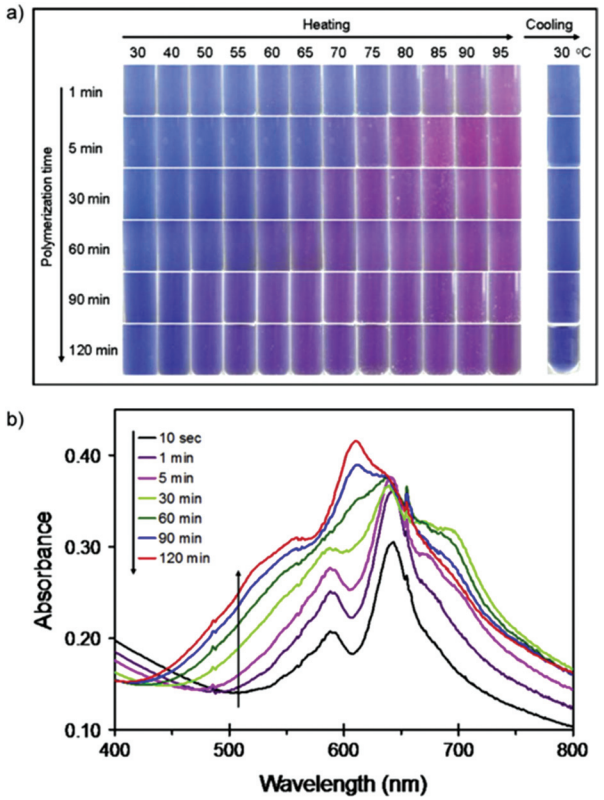

Fig. 4 (a) Photographs of the thermochromic transition of PDA/ZnO composites with varied photopolymerization time observable by the naked eye. PDA/ZnO composites were heated from 30 °C to 95 °C, and cooled back to 30 °C, showing reversibility. (b) UV-Vis absorption spectra of PDA/ZnO nanocomposites as a function of irradiation time. Reproduced from ref. 29 with permission from Elsevier, copyright [2015].

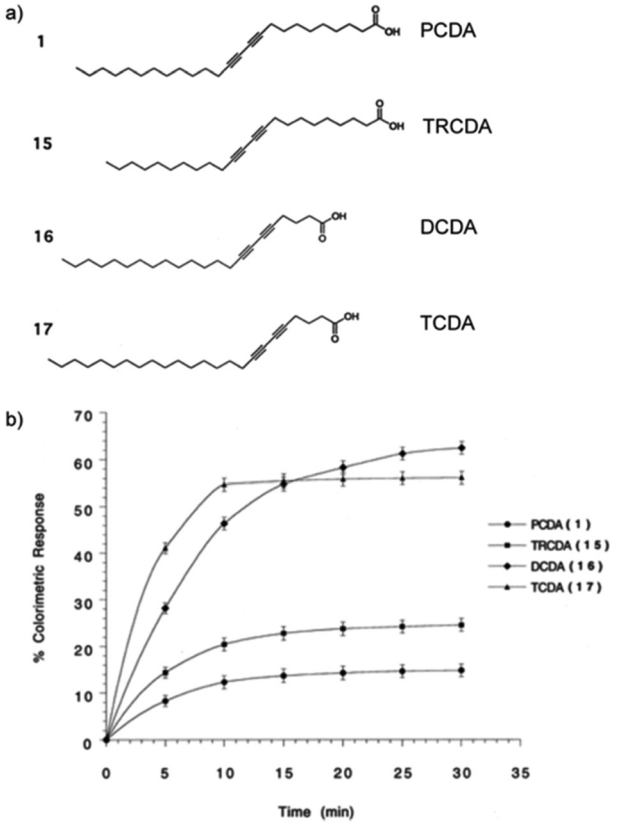

Fig. 5 (a) Chemical structure of 10,12-pentacosadiynoic acid (PCDA), 10,12-tricosadiynoic acid (TRCDA), 5,7-docosaciynoic acid (DCDA), and 5,7-tetracosadiynoic acid (TCDA). (b) Thermochromic colorimetric response of PDA vesicles composed of the different DA monomers after incubation at 50 °C as a function of time. Reproduced from ref. 30 with permission from the American Chemical Society, copyright [1998].

state. The change of strain within the PDA backbone plays an important role on the chromic reversibility. Thus, to ensure optimized PDA nanosensor synthesis conditions, a trade-off between the chromic transition temperature and irreversibility should be made.

Despite the enhanced sensitivity achieved by optimization of photopolymerization time, the sensitivity of the system is increased to environmental stimulus such as heat and reduced thermochromic reversibility. Although an increase in sensitivity towards chemical recognition is also reported, the increase in sensitivity is non-specific and may inhibit out of lab application. As a result, optimizing photopolymerization time should consider other sources of stimulus present in the desired application.

Alkyl chain length

Typical DA monomers have two alkyl chains: an alkyl spacer that separates the diacetylene functional group from the head group, and an alkyl tail (Fig. 5a). Adjusting the length of these carbon chains is a common method of sensitivity control. Okada *et al.* systematically varied the length of the alkyl chains in diacetylene monomers to observe the effect on colorimetric response in PDA vesicles.[30] The comprehensive work studied seventeen monomers with different structures and observed their ability to self-assemble into polymerizable vesicular structures. Transmission electron microscopy and dynamic light scattering were performed on systems of stable vesicles. It was found that particles with large bulky head groups did not form polymerizable vesicles with regular morphology. The colorimetric response of four carboxy-terminated DA derivatives (10,12-pentacosadiynoic acid, 10,12-tricosadiynoic acid, 5,7-docosaciynoic acid, and 5,7-tetracosadiynoic acid) were studied as a function of time at a constant temperature of 50 °C (Fig. 5b). A relationship between the thermochromic sensitivity and the positioning of the diacetylene functional group along the length of the alkyl chain was reported. The colorimetric response of 5,7-monomers is six times greater than 10,12-monomers.

This phenomenon is well explained by comparison of the cohesive energy of the alkyl chain separating the diacetylene functional group and the carboxylic acid head group. The 5,7-derivatives have a C-3 alkyl chain (cohesive energy = 20 kJ mol^{-1}) while 10,12-derivatives have a C-8 alkyl chain (cohesive energy = 55 kJ mol^{-1}). It is proposed that the longer more rigid C-8

chain stabilizes the conjugation associated with the blue phase, thereby reducing thermochromic sensitivity. The overall chain length of the molecules is also shown to influence conjugation stability and thermochromic sensitivity. Longer chain diacetylene molecules of the same diacetylene positioning are stabilized from an increase in dispersion forces. However, the positioning of the diacetylene functional group has a dominant influence on thermochromic sensitivity over total chain length. This trend was also observed in the detection of a cholera protein toxin with mixed PDA G_{M1} Ganglioside toxins. 5,7-Docosadiynoic acid (DCDA; 20 carbon atoms) was found to be more sensitive in toxin detection than 10,12-pentacosadiynoic acid (PCDA; 25 carbon atoms).[30,34] This is attributed to the shorter length between the head group and the diacetylene group, increasing the association of the recognition element with the diacetylene transducer.

Charoenthai *et al.*[35] studied the impact of alkyl tail length on the colorimetric response of PDA vesicles to temperature, ethanol, and pH with findings that support the trends found by Okada *et al.*[30] They reported a complete color change in PCDA at 65 °C and a complete color change of 10,12-tricosadiynoic acid (TCDA; 23 carbon atoms) at 60 °C. TCDA only required 40% (v/v) ethanol to induce full color change where PCDA required 55% (v/v) ethanol. Similarly, TCDA (pH 8.5) required a smaller increase in pH to PCDA (pH 9) to undergo color change. These three trends were attributed to the shorter alky tail of TCDA, which contribute smaller dispersion forces to conjugation stability. Chanakul *et al.*[36] observed similar results when studying the effect of alkyl chain length on the thermochromism of PDA/ZnO nanocomposites. The shortening of the alkyl side chain led to a systemic decrease in color transition temperatures (Fig. 6).

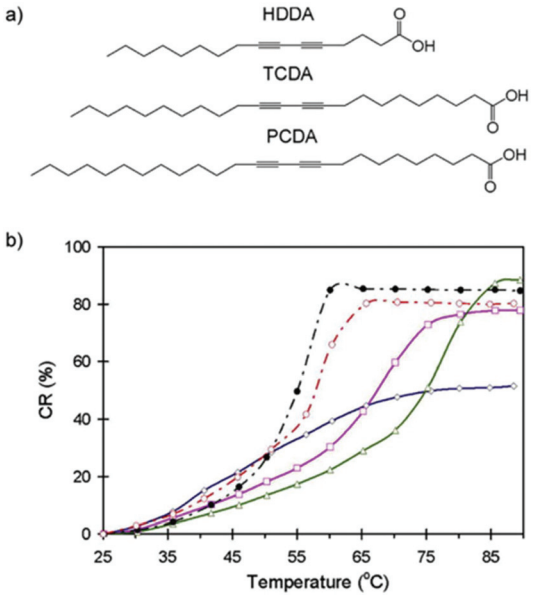

Fig. 6 (a) Chemical structure of DA monomers used to construct PDA/ZnO nanocomposites and (b) colorimetric response (CR) as a function of temperature. Symbols are for poly(PCDA) (○), poly(TCDA) (●), poly (PCDA)/ZnO (△), poly(TCDA)/ZnO (□), and poly(HDDA)/ZnO (◊) nanocomposites. Reproduced from ref. 36 with permission from Elsevier, copyright [2013].

However, Kim *et al.* found that a PDA-based sensing characteristics could not be tuned by manipulation of alkyl chain length if the head group had dominant intermolecular forces.[37] PDA-mBzA liposomes constructed from PCDA (25 carbon atoms), 4,6-heptadecadiynoic acid (HDCDA; 19 carbon atoms), 5,7-eicosadiynoic acid (ECDA; 18 carbon atoms), and 8,10-heneicosadiynoic acid (HCDA; 17 carbon atoms) exhibited reversible color changes at the same temperature. Despite the structural differences of each of the PDA systems, the length of the alkyl chain was found to have no impact on the chromatic reversibility and color transition temperature of each PDA-mBzA derivative. The high degree of hydrogen bonding in PDA-mBzA leads to very strong interactions between head groups, overpowering other intermolecular forces in the structure. Similarly, Wu *et al.* formed hydrogen bonded complexes of poly(4-vinlypryidine) and PDAs for volatile organic compound (VOC) sensing with TCDA and 4,6-heptadecadiynoic acid (HDDA).[38] Despite the HDDA derivatives having a much smaller alkyl spacer length than the TCDA, their colorimetric response to organic solvents were comparable, indicating their sensitivity was dominated by the properties of the head group.

Jiang *et al.* developed a thin film PDA colorimetric microarray sensor for VOCs.[39] PDA-based micro patterns were fabricated by a sol–gel process and soft lithography using PCDA, TCDA, and other head group modified PDA derivatives. The array was able to detect and discriminate between six different VOCs including dimethyl formamide (DMF), cyclopentanone, toluene, ethanol, cyclohexane, and acetonitrile. The authors reported that films derived from TCDA were the most sensitive to VOC detection and displayed color transitions to all compounds except acetonitrile. However, PCDA films exhibited comparable or higher colorimetric responses when exposed to three of the six tested compounds (Fig. 7). These results suggest that the impact of the alkyl tail length is lesser in films than when organized in vesicular structures.[30]

Kamphan *et al.* also found that the dependence of PDA sensitivity on alkyl chain length was different in films than vesicular structures.[40] Intercalated PDA/polyvinylpyrrolidone (PVP) films were constructed *via* a solvent casting method using a range of DA mixed with PVP in ethanol. Decreasing the alkyl tail length was found to reduce the color change temperature from 85 °C to as low as 75 °C which was attributed to a decrease in dispersion forces. However, reducing the alkyl spacer length between the carboxylic acid head group and the diacetylene group was found to have little impact on the color transition temperature. This is different to the behavior reported in liposomes where the alkyl spacer is the predominant influence on sensitivity.[30] The authors explained that the local interactions near the carboxylic head group are strong due to intercalation with PVP, stabilizing the head group and diacetylene group. The expected decrease in dispersion forces from the reduction in alky spacer length is masked by PDA–PVP stabilizing forces and has negligible effect on the color transition temperature.

a)

% CR	DMF	cyclopentanone	toluene	ethanol	cyclohexane	acetonitrile
TCDA	68	71	50	21	7	0
PCDA	73	78	42	24	0	0
PAPCDA	12	27	15	0	8	0
CNAPCDA	0	0	2	0	0	0

b)

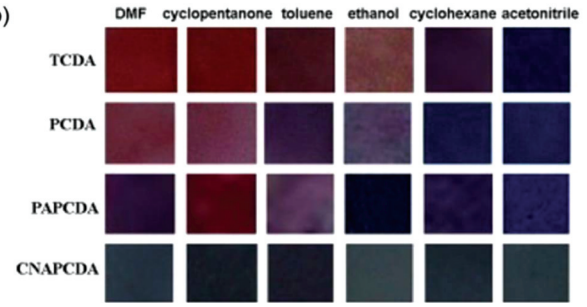

Fig. 7 (a) Colorimetric response and (b) photographs of PDA-embedded polymer matrix films derived from TCDA, PCDA, PAPCDA, and CNAPCDA after exposure to organic solvents at room temperature. Reproduced from ref. 39 with permission from Elsevier, copyright [2010].

Khanantong *et al.* have recently completed a study on PDA vesicles constructed from seven different monomers.[41] They systematically altered the chain length of the alkyl tail and alkyl spacer between the carboxylic head and diacetylene group (Fig. 8). Reducing the alkyl tail was found to reduce color transition temperature in agreement with earlier reports.[30] However, they found that reducing the alkyl spacer length between the carboxylic head group and the diacetylene group increased the temperature required for color transition. This is the opposite trend observed by Okada *et al.* in vesicular structures.[30] They suggest that the shortening of the alkyl segment reduces the dispersion interaction within the PDA assemblies, however the dynamics of the carboxylic head group is restricted. Rather than increasing the association of the head group with the diacetylene group as previously claimed, they suggest that reducing the alkyl spacer reduces the head group mobility, stabilizing the molecules conjugated segment.

The literature indicates that manipulating the length of the alkyl chains in DA monomers is an effective way to control PDA sensing characteristics. The effects of these modifications are stronger when PDA is organized in vesicular structures.

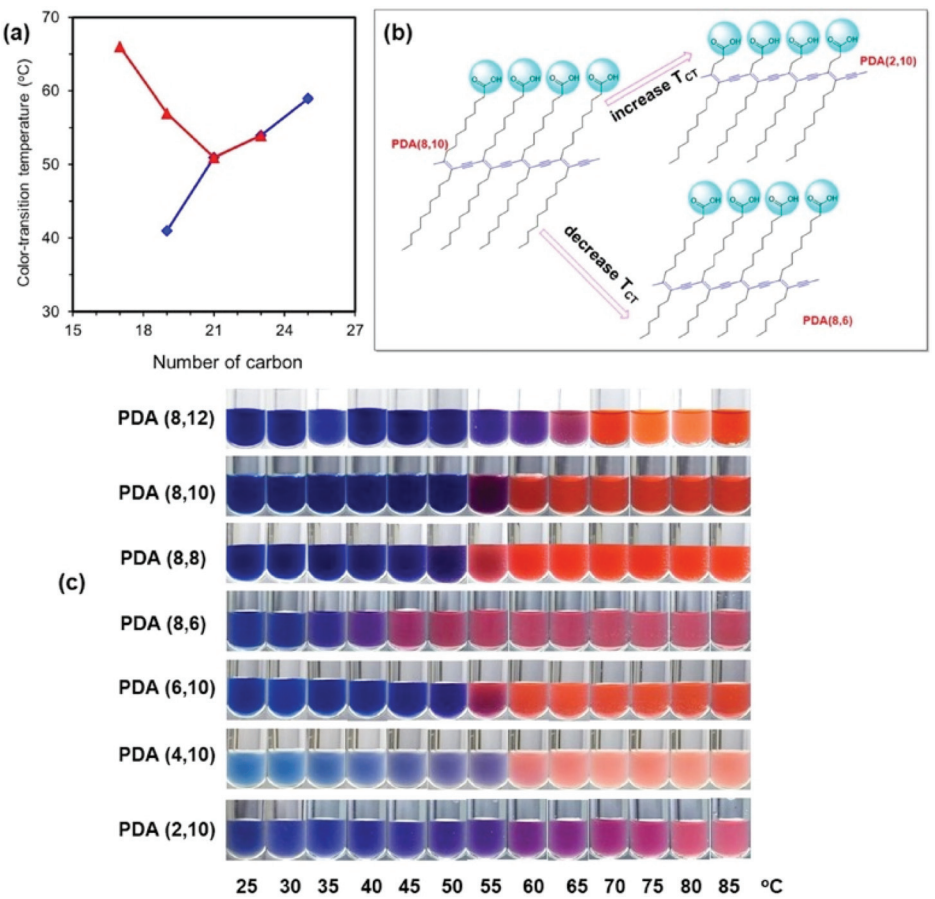

Fig. 8 (a) Plots of color transition temperature (T_{CT}) *versus* number of carbon within the repeating unit of PDAs. Symbols are for (◆, blue) PDA(8,*y*) and (▲, red) PDA(*x*,10). (b) The opposite change of T_{CT} when the alkyl segments at different regions are shortened. (c) Color photographs of PDAs in aqueous suspension taken upon increasing temperature. Reproduced from ref. 41 with permission from Elsevier, copyright [2018].

However, below a certain size, the decrease in dispersion forces associated with short chain DAs inhibits spontaneous assembly into stable vesicles with regular morphology.[30] In these instances, films may be a more suitable arrangement.

To conclude, studies have demonstrated that shortening the alkyl tail length of DA monomers could improve the thermochromic sensitivity by decreasing the color transition temperature. However, in the face of strong intermolecular forces between PDA head groups, or when the PDA nanosensors are in different format, the manipulation of alkyl tail length to improve PDA sensitivity may be made redundant. Thus, to ensure that the alkyl chain length modification is effective, it is essential to take into account the inherent relationship between the positioning of diacetylene functional group along the alkyl length and the thermochromic sensitivity.

Head group modification

Apart from the total chain length and the position of the diacetylene compound within the chain, chemical properties of the diacetylene unit is of utmost importance for signal amplification in PDA-based sensors.[32,42] During polymerization, the long alkyl chains and functional head groups within the diacetylene monomers self-assemble due to strong intermolecular interactions in the hydrophobic tail, π-orbital stacking, hydrogen and ionic bonding.[43] Owing to this self-assembling property, the extent of the delocalized π-conjugation and conformational restriction of the PDA suprastructure which affect the PDA-based sensor sensitivity and stability could be effectively tuned by modifying the head groups.

Several studies have reported that the sensitivity of PDA sensors can be effectively improved by modifying the intermolecular forces between the neighboring diacetylene molecules and their head groups.[29,31,32,44,45] Starting with PDA for thermo-sensing, the temperature sensitivity and reversibility vary depending on its intended use, which means that the design of PDA thermosensors should be tuned according to its application. For example, Mapazi *et al.* synthesized PDA thermosensors for repeated high temperature sensing and monitoring,[46] which means that thermochromic reversibility is essential. High-temperature sensing is particularly useful for goods that require fusing. The challenge to this work was that PDA chain melts at moderate temperature (>40 °C) and the thermochromism is irreversible above 60 °C.[29] To overcome this limitation, the authors functionalized urea to the head group of PCDA to provide hydrogen bonding sites which strengthen the head groups interaction. Differential scanning colorimetry results showed that the formation of *N*-acylurea from the addition of urea increased the melting point of pure PCDA 47.29 °C to 151.87 °C. Thermogravimetric analysis further proved that the thermal stability was improved from 63.65 °C to 315 °C. It was hypothesized that the strong electrostatic interactions between the head groups provided a thermal jacket for the π-conjugated backbone protection against heat stress.

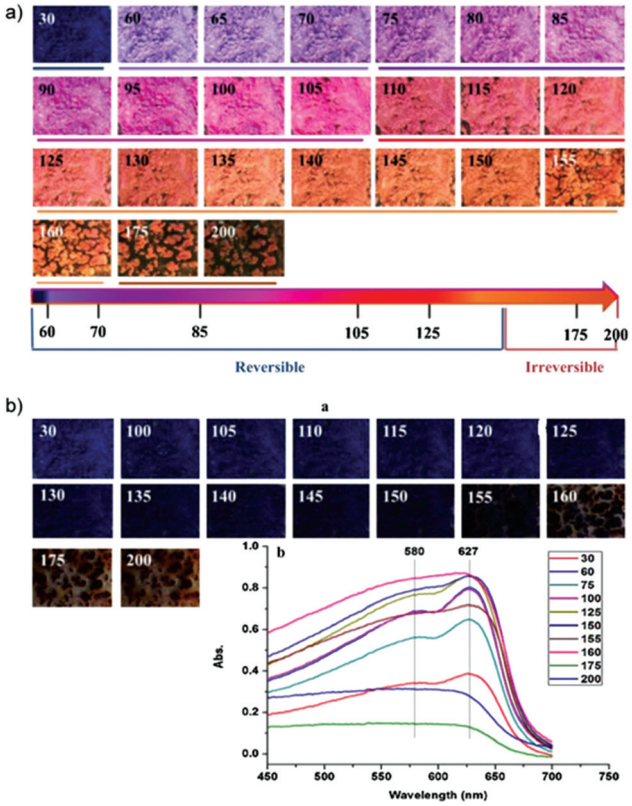

Fig. 9 (a) Photographs of PDA-urea at temperatures ranging from 30 to 200 °C post-2 minutes equilibration. The color transition path with its reversibility upon heating is represented as the rainbow line. (b) Photographs of PDA-urea powders at room temperature after cooling. Reproduced from ref. 46 with permission from Elsevier, copyright [2017].

Fig. 9a depicts the color-transition phases of PDA-urea powder when heated up to 200 °C and cooled (Fig. 9b) to room temperature. At temperatures above the melting point of 150 °C, PDA-urea powder no longer exhibited reversible thermochromism as confirmed by UV-Vis spectra results whereby the 580 nm peak was no longer distinguishable (Fig. 9b). It was further shown that above 150 °C, the powder morphology began to alter as particles fuse and form agglomerates from melting and solidify upon cooling. As the long alkyl chains melt and overlap into the geometrical spaces of the neighboring molecules, intermolecular entanglements disturbed the electronic conjugation length and the crystalline geometries collapsed from the increased *d*-spacing within the PDA crystals. Overall, the authors successfully fabricated urea-modified PDA thermosensor with high-temperature sensing and reversible thermochromism up to 150 °C.

On the flipside, Park *et al.* explored the fabrication of low temperature thermochromic PDA sensors to display color transitions from 5–30 °C for its potential use in refrigerated or frozen goods.[47] In contrast to Mapazi *et al.*,[46] an irreversible PDA sensor is important for Park *et al.*[47] so to indicate materials' exposure to high temperature during transport or storage. The challenge to this work was again attributed to the

fact that PDA transition temperature is typically above room temperature, around 40 °C. Park *et al.*[47] was able to lower the melting point of resulting PDA nanosensors to −5 °C by incorporating methyl or methoxyethyl ester groups which removed the strong headgroup interactions. The authors also compared the performance of ester polymerized-PDAs with different alkyl chain length made from three diacetylenic acids precursors: PCDA (melting point at 62–63 °C), TCDA (melting point at 54–56 °C), and HCDA (melting point at 51–52 °C). Fig. 10a illustrates the preparation scheme of these PDA thermosensors. Each DA precursor underwent esterification reactions with MeOH in the presence of 1-ethyl-3-3(3-(dimethylamino) propyl)carbodiimide (EDC) and (dimethylamino)pyridine (DMAP) to produce -Me sensors. 2-Methoxyethanol were used to generate -EGME sensors. The CR plotted in Fig. 10b shows the characteristic temperature ranges when CR values rocketed: 28–29 °C (PCDA-Me), 21–24 °C (PCDA-EGME), 15–18 °C (TCDA-Me), 10–12 °C (TCDA-EGME), 7–10 °C (HCDA-Me), and 2–5 °C (HCDA-EGME). It was found that these ranges were strongly correlated to the melting point of each corresponding monomers, with lower transition temperature on shorter chain length and -EGME sensors consistently showing color change at lower temperature when compared to -Me sensors. It was also reported that the lesser the methylene groups between the DA and the terminal methyl group (*m* value), the weaker the intermolecular interactions. Thermochromic transition temperature decreased by 10 °C when the alkyl chain length is shorter by two methylene units.

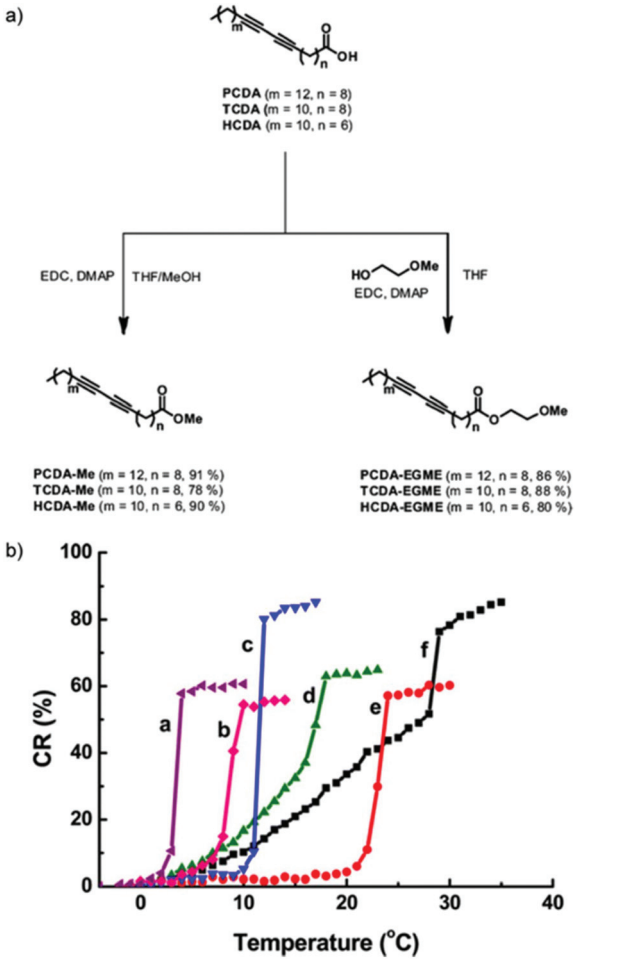

Fig. 10 (a) Schematic diagram of the preparation of diacetylene monomers to produce low temperature thermochromic PDA nanosensors. (b) Colorimetric response (CR) plot as a function of temperature of PDAs functionalized with ester moieties; (a) HCDA-EGME, (b) HCDA-Me, (c) TCDA-EGME, (d) TCDA-Me, (e) PCDA-EGME, (f) PCDA-Me. Reproduced from ref. 47 with permission from the American Chemical Society, copyright [2016].

Wang *et al.* designed a highly sensitive and selective PDA-based sensor derived from 1-(1,4,7,10,13-pentaoxa-16-azacyclooctadec-16-yl)-pentacosa-10,12-diynamide (PCDA-L) and PCDA for Pb^{2+} detection in aqueous HEPES buffer solution.[48] The sensor selectivity was evaluated in the presence of the perchlorate salts of Cu^{2+}, Na^{+}, Hg^{2+}, Fe^{3+}, Mn^{2+}, Cr^{3+}, Co^{2+}, Zn^{2+}, Mg^{2+}, Li^{+}, Ni^{2+}, Cd^{2+}, Ag^{+}, and Al^{3+}. The colorimetric response of poly-PDA-L in Fig. 11a showed the selective and clear phase transition from blue to red in the presence of Pb^{2+}, whereas no color change was observed in pure PDA vesicles (Fig. 11b). The quantitative CR in Fig. 11c showed a gradual increase from 0–6 μM Pb^{2+}, before reaching a plateau at a CR% value of 71.2%. Although not mentioned in the article, this plateau may have been correlated to the 3 : 7 molar ratio of the PCDA-L and PCDA used to synthesize the composite. The colorimetric transition was due to the interaction of Pb^{2+} with tween 1-aza-18-crown 6-ether moiety, which induced strain on the alkyl side chains of the PDA backbone and thus generating the color change. The detection limit of this sensor was found to be at 1 mM Pb^{2+} as calculated through microscopy using cellSens software.

Lipid doping

Biological cells have a lipid-based membrane that creates a barrier between intracellular components and the extracellular environment. The membrane is decorated with proteins and glycoproteins that enable the cell to monitor and respond to the external environment (Fig. 12). Doping PDA vesicles with lipids to create synthetic mimics of biological cells has become a popular method to construct colorimetric biosensors. Similar to biological cells, these synthetic mimics can also be decorated with recognition elements to target specific analytes. Adopting the spherical cell structure is advantageous over bilayer films as it provides a three-dimensional interface with its environment and organizes and orients recognition elements favorably. The lipid component of the mixed vesicle can serve as a recognition element or it can be used to tune membrane properties to control sensor performance.

Lipid doping of PDA vesicles has been demonstrated as an effective recognition strategy for pore forming toxins excreted from haemolytic bacteria. The lipids and diacetylene monomers arrange themselves into separate and alternating lipid and DA moieties that allow photopolymerization to form blue

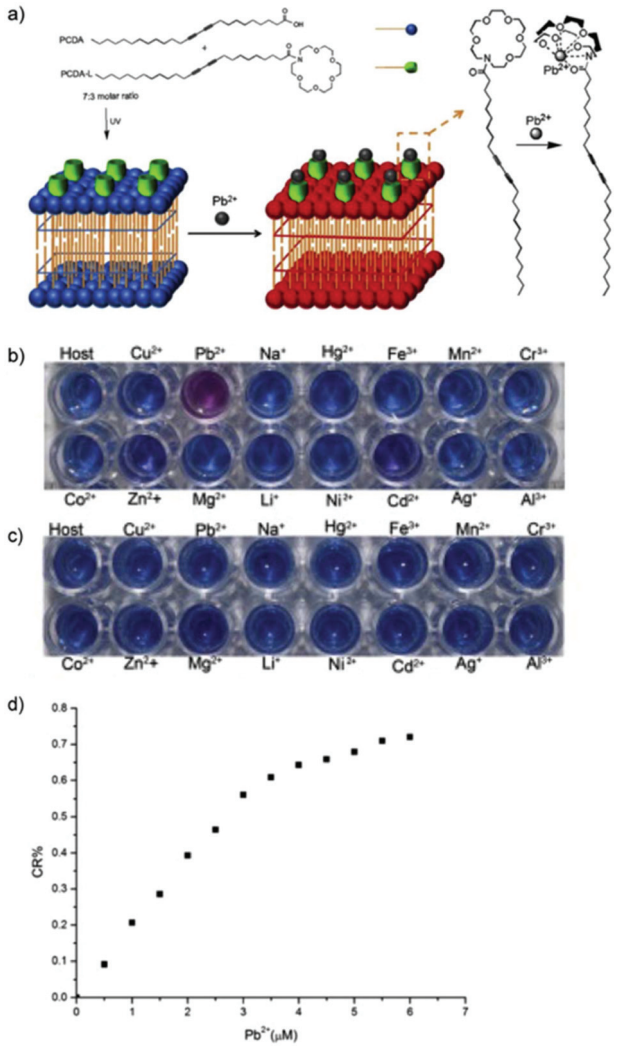

Fig. 11 (a) The synthesis and binding mechanism of poly-PDA-L with Pb^{2+}. PCDA-L and PCDA was mixed at 3 : 7 molar ratio. Digital images of the colorimetric responses of (b) poly-PDA-L and (c) pure PDA vesicles towards various metal ions (10 μM) in HEPES buffer. (d) Colorimetric response (CR%) of poly-PDA-L at different Pb^{2+} concentrations in HEPES buffer. Reproduced from ref. 48 with permission from Elsevier, copyright [2015].

phase PDA. Upon exposure to bacterial secretions, the haemolytic toxins form pores in the lipid moiety which induces a structural disturbance in the vesicle membrane. This creates a perturbation in the conjugated backbone of the PDA moiety and an observable blue to red color change allowing indirect detection of pathogenic bacteria. An extensive documentation of PDA/lipid systems for the detection of haemolytic bacteria and toxins exists in LeBègue *et al.*'s recent review on PDA vesicles for biosensing microorganisms.[7] As a result, this review will only discuss work that details the impact of lipid constitution upon the sensitivity of lipid doped PDA vesicles.

Lipid doping of PDA vesicles was first reported by Jelinek where he reported DMPC formed subdomains in the DA membrane that still enable photopolymerization to form a PDA

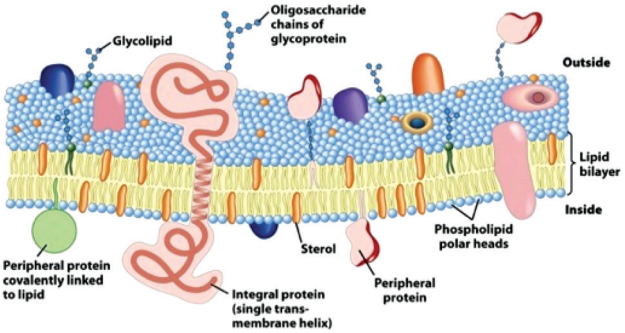

Fig. 12 An illustration of the fluid mosaic model for the biomembrane structure. Carbohydrates, lipids, and proteins decorate the surface of the membrane and are the sites of specific molecular recognition interactions that are transduced into cellular messages. Reproduced from ref. 49 with permission from W H Freeman & Co, copyright [2000].

composite. Within the Jelinek's research group, Scindia *et al.* went on to construct a sensing system capable of detecting and discriminating between a range of bacterial analytes.[5] The arrayed test is constructed from TCDA that is doped with four different mixtures of lipids: DOPE, sphingomyelin, DMPC, and POPG. Each system exhibits a unique colorimetric response to the supernatants of *E. coli*, *B. Cereus* and *S. typhimurium*. Colorimetric responses between 20% and 80% red chromatic shift were observed, which were attributed to interaction between bacterially secreted molecules and the lipid component of the sensor. Different types of bacteria excrete a unique and characteristic profile of substances that play functional roles in bacterial proliferation.[50] Many of these substances, such as exotoxins (*e.g.* alpha-hemolysin) and endotoxins (*e.g.* lipopolysaccharides) are membrane active and form pores in phospholipid membranes.[51] The authors attribute the unique colorimetric fingerprint to the characteristic profile of excreted substances from each bacterium, allowing their discrimination (Fig. 13). They also nominate that the phospholi-

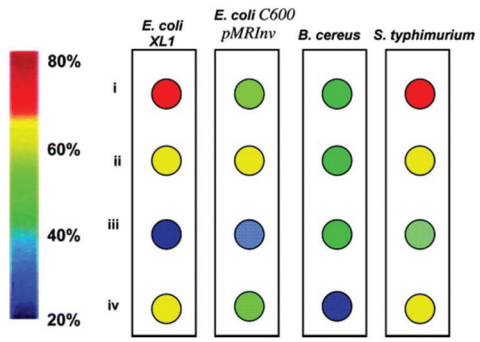

Fig. 13 Colorimetric bacterial fingerprinting. The color combination for each bacterium reflects the red chromatic shift (RCS) values recorded 7 h after the start of growth at a bacterial concentration of 1×10^9 mL^{-1}. The RCS color key is shown on the left. (i) DOPE/PDA (1 : 9 mole ratio); (ii) sphingomyelin/cholesterol/PDA (7 : 3 : 90); (iii) DMPC/PDA (1 : 9); and (iv) POPG/PDA (1 : 9). Reproduced from ref. 5 with permission from the American Chemical Society, copyright [2007].

pids different head groups, size, structure and surface charges dictate the sensitivity of each respective systems response to haemolytic toxins in the supernatant. However, no specific explanations are provided as to why some lipid constitutions are more sensitive to some secretions and not others. The ability of the array to discriminate between different types of bacteria is also limited to a small concentration range (10^6 particles per ml). However, the results highlight the ability to tune to the color response of PDA systems by doping with different lipids to serve as a recognition element.

Kang *et al.* synthesized PDA-epoxy liposome assemblies containing phospholipids that have different head group charges and phase transition temperatures (T_m) to observe their impact on the systems sensing performance.[52] Electrophoretic light scattering measurements indicated that phospholipids with strong positive (DMTAP) or negative (DMPA) charges helped to stabilize liposome solutions by increasing the magnitude of the particle's zeta potential. Strong surface charges create repulsive forces that inhibit aggregation, stabilizing the particles in solution for over one week. DMPC, a zwitterionic phospholipid, reduced the stability of solutions by neutralizing the particles zeta potential. This led to particle aggregation after just four hours. A relationship between liposome morphology and phospholipid doping was observed by transmission electron microscopy (Fig. 14a) and thermochromic testing (Fig. 14b). Incorporation of phospholipids with a high magnitude charge and moderate T_m (DMPA, T_m = 50 °C) led to small liposomes with regular morphology and lower thermochromic transition temperatures. Liposomes doped with phospholipids with a low melting temperature, DMPC (T_m = 23 °C) and DMTAP (T_m = 20–24 °C), led to a larger rectangular morphology with decreased thermochromic sensitivity.

The PDA-phospholipid liposomes were then utilized in an immunoassay to detect Bovine Viral Diarrhea Virus (BVDV). An indirect detection system was designed that used the BVDV antigen as a probe to detect the BVDV IgG antibody. The PCDA/DMPC system was excluded from this due to its instability in solution. Fig. 15 illustrates the correlation curve between the colorimetric response and the concentration of BVDV antibody after 24 hours incubation in the antibody solution, reinforcing that phospholipids with a moderate T_m and high magnitude charge produce smaller more regular liposomes with a greater sensitivity to biological recognition events. Although the test is able to detect BVDV, the maximum colorimetric response observed in this test is only ~10%, which is relatively low compared to other PDA based sensing systems. Nomura *et al.* have used a similar method to control the morphology of DOPC liposomes by cholesterol doping, radically reducing their liposome size.[53]

Guo *et al.* have demonstrated mechanical control over morphology and sensing characteristics of glycolipid-doped PDA vesicles *via* mechanical extrusion.[54] Passing the liposomes through a series of membranes with different pore sizes they synthesized liposomes with 1 μm, 0.45 μm and 0.2 μm diameters. The liposomes were used to detect concanavalin A, a

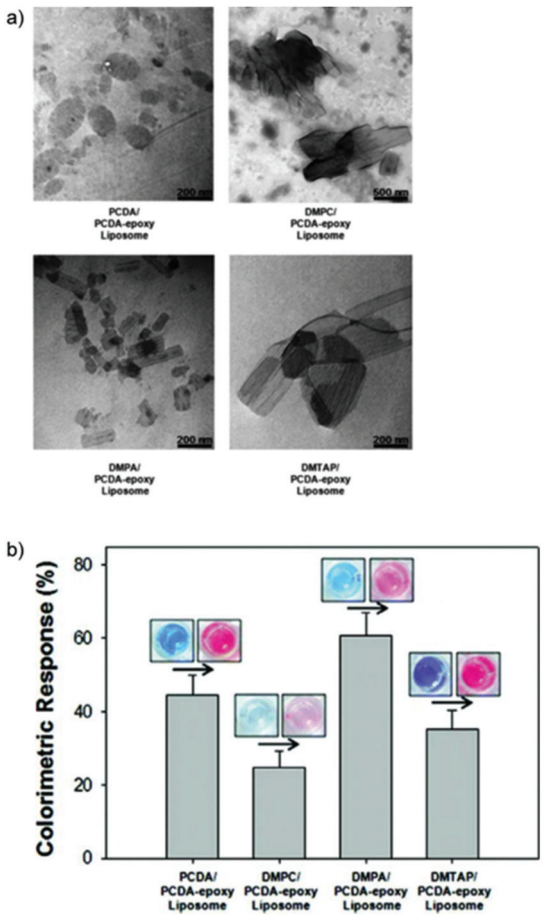

Fig. 14 (a) Transmission electron microscopy images of the different PDA-phospholipid liposomes. (b) Colorimetric response of PDA-phospholipid liposomes after 254 nm UV polymerization for a series of time periods and heating at 70 °C. Reproduced from ref. 52 with permission from the American Chemical Society, copyright [2012].

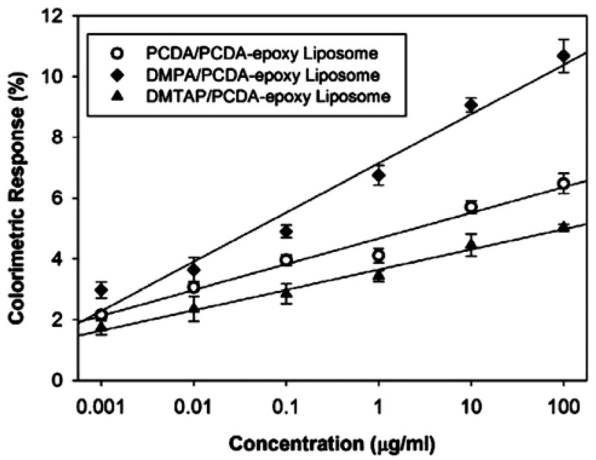

Fig. 15 Colorimetric response of PDA-phospholipid liposomes as a function of concentration of BVDV antibody. Reproduced from ref. 52 with permission from the American Chemical Society, copyright [2012].

lectin of the jack bean that binds to glycolipids. It was reported that decreasing the PDA-glycolipid size increased the systems' sensitivity towards concanavalin A. This suggests that the increase in sensitivity observed by Kang *et al.*[52] when doping PDA morphology can be achieved *via* mechanical control over vesicle size. More recently Kim *et al.* have demonstrated morphological control with a more sophisticated microfluidic chip scheme.[55] Adjustment of the flowrate of the DA monomers and DI water pumped through the chip allows better control over PDA size with a narrower size distribution than what can be achieved *via* extrusion.

Okada *et al.* reported the impact of lipid doping on PDA membrane flexibility very early.[30] They incorporated sialic acid ligands in vesicles at 5 : 95, 20 : 80 and 40 : 60 ratios of sialic acid : TCDA. Upon increasing the sialic acid concentration from 5% to 40% the CR% linearly increased from 50% to 90% in response to a temperature to 50 °C due to an increase in membrane flexibility. More recently Kim *et al.* conjugated antibodies to PDA vesicles *via* biotin–avidin complexes which were immobilized on glass slides.[56] Vesicles that were doped with 20–30% DMPC had drastically reduced response times for color and fluorescence changes which were optimal properties for bacterial detection. Fourier Transform Infrared spectra analysis suggested that DMPC insertion decreased hydrogen bonding between amide and carboxylic acid groups on neighboring PDA head groups throughout the liposome. This increased the membrane flexibility allowing more rapid detection of molecular recognition events.

Doping PDA with lipids has been shown to give control over sensitivity by two methods: (1) tuning morphology which impacts sensor performance and (2) increasing membrane flexibility by interrupting intermolecular forces between PDA head groups. Although these methods may be suitable for some applications, they typically increase the sensitivity of the system to environmental stimulus such as light, temperature and pH along with the targeted analyte. For out of lab applications, lipid doping does not serve as an ideal method to tune PDA sensor characteristics due to a decrease in specificity.

Metal and non-metal oxide composites

Combining PDA with metal oxides to form nanocomposites has been shown to have an interesting impact on PDA sensing characteristics. Patlolla *et al.* sonicated ZnO, TiO_2, and ZrO_2 with PCDA in chloroform before evaporation to form PDA/metal oxide powders.[57] Thermochromic testing revealed that PDA/ZnO nanocomposites exhibited higher color transition temperatures and rapid reversibility, whereas nanocomposites containing TiO_2 and ZrO_2 were irreversible. The color change mechanisms were explored using Raman spectroscopy, FTIR, DSC and XAFS. In pure PCDA, heating induces an irreversible strain on the polymer backbone. In PDA/ZnO, results indicate a chelation between the carboxy head groups of the PCDA and the surface of the ZnO particles. The attractive forces can alleviate thermal strain on the backbone and restore the blue phase PDA upon cooling.

Wu *et al.* made TCDA/ZnO nanocomposites *via* the same technique to observe the effect of ZnO concentration on the thermochromic behaviour.[58] Pure TCDA exhibited a completely irreversible color change whilst 5 wt% ZnO nanocomposites showed a partially reversible color change. ZnO concentration of 10 wt% and 15 wt% had higher color transition temperatures and exhibited completely reversible thermochromism (Fig. 16), which was also attributed to chelate formation.

Wu *et al.* went on to explore PCDA, TCDA, and 10,12-docosadiynedioic acid (DCDA)/ZnO nanocomposites as potential sensors for organic liquids.[58] The powdered nanocomposites sensitivity to organic liquids was lesser than pure PDAs due to the stabilizing interactions between the carboxylic head groups and ZnO particles. They also demonstrated the ability to inkjet print PDA/ZnO nanocomposites onto paper substrates (Fig. 17) while maintaining reversible thermochromic behaviour.[59,60]

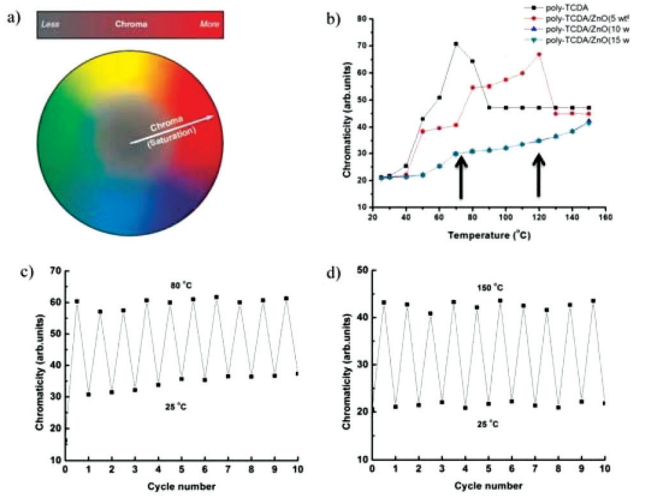

Fig. 16 (a) Schematic showing chromaticity distribution from dull to vivid. (b) Chromaticity *versus* temperature plots for TCDA and TCDA/ZnO composites. (c) Chromaticity of TCDA/ZnO (5 wt%) as a function of thermal cycle. (d) Chromaticity of TCDA/ZnO (15 wt%) as a function of thermal cycle. Reproduced from ref. 58 with permission from the American Chemical Society, copyright [2013].

Fig. 17 QR code with partial area of TCDA/ZnO fabricated by inkjet printing methods to serve as a time temperature indicator. Reproduced from ref. 59 with permission from Elsevier, copyright [2014].

Chanakul *et al.* synthesized nanocomposite PDA/ZnO liposomes in aqueous solution *via* the hydration of DA dry films under sonication with 10 wt% ZnO solution.[36] They observed the effect of varying the alkyl chain length of the DA monomer on the thermochromism of the PDA/ZnO nanocomposites. Longer chain DA monomers (PCDA and TCDA) had stronger and more homogenous interfacial interactions with ZnO, which led to higher color transition temperatures and better chromatic reversibility. Shorter chain DA monomers (HDDA) had lower color transition temperatures and only exhibited partial reversibility.

Chanakul *et al.* studied the colorimetric response of PDA/ZnO to both acids[61,62] and bases.[61] Pure carboxy-terminated PDA does not change color in response to acids. The authors realized that exposing PDA/ZnO nanocomposites to low pH led to the dissociation of the ZnO nanoparticles and a corresponding blue to red color transition.[61] The color change is a result of the destruction of steric forces between PDA head groups and ZnO, resulting in an irreversible color transition. The pH at which these nanocomposites exhibit a color change can be tuned by altering the structure of the diacetylene monomer. Chanakul also found that the structure of acid analytes played an important role in the sensitivity of the color response.[62] It was also found that ZnO stabilized the conjugated backbone of PDA in the face of an increasing pH. Carboxy-terminated TCDA changes from blue to red between pH 8 and 9. When combined into a TCDA/ZnO nanocomposite, the pH of color transition is extended to pH 13, a result of stabilizing attractive forces between the ZnO particle and PDA headgroups (Fig. 18). These forces also stabilize PDA/ZnO in organic solvents 1,2-dichlorobenzene, chlorobenzene, toluene, ethanol, butanol, hexanol, chloroform and tetrahydrofuran.[63] This allows the PDA nanocomposite to be combined with common polymers such as poly(styrene), poly(methyl methacrylate), poly(ethylene) and poly(vinyl alcohol) by using a simple solvent mixing process which is not possible with pure PDA.

PDA can be combined with silica to form nanocomposites to enhance thermochromic stability and reversibility. Similar to PDA/ZnO, PDA/silica systems rely on attractive forces between silica surface charges and PDA head groups. Peng *et al.* synthesized PDA/silica nanocomposites by covalent bonding to silica frameworks, providing control over molecular alignment and stability.[64] The molecular architecture could be tuned by controlling conjugation to influence the mesostructure and chromatic response. Covalent interactions between silica and PDA increased the reversible chromatic transition temperature from 70 °C to 113 °C. Employing a different strategy, Nopwinyuwong *et al.* synthesized PDA vesicles with silica core particles.[65] Attractive forces between the surface of the silica particle and the PDA carboxylic head groups increased thermochromic stability and reversibility which could be tuned by the adjustment of the silica concentration. More recently Wang *et al.* have synthesized PDA-based periodic mesoporous organosilica films with different molar fractions of diacetylene bridged silsesquioxane.[66] The films have a multi-step and reversible thermochromic color transition,

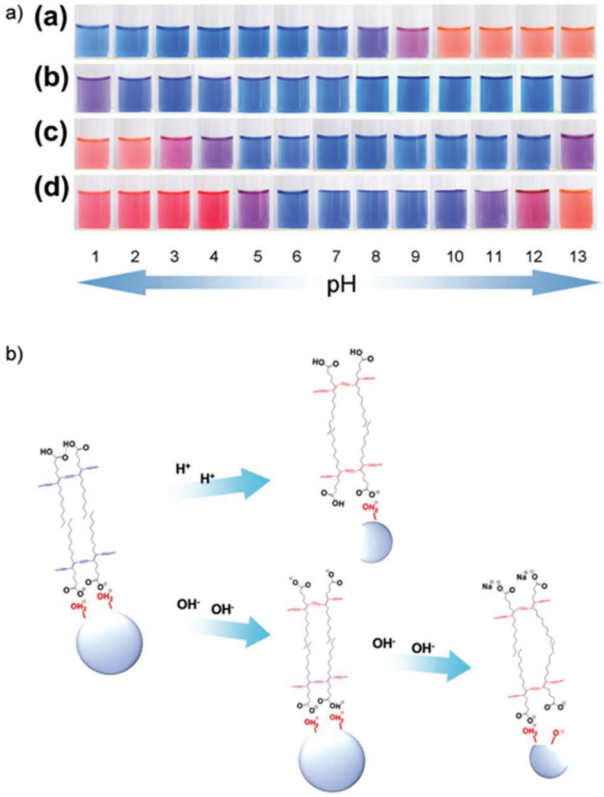

Fig. 18 (a) Photographs of aqueous suspensions of (a) pure poly (TCDA), (b) poly(PCDA)/ZnO (c) poly(TCDA)/ZnO, and (d) poly(HDDA)/ZnO nanocomposites taken at different pH. (b) The ZnO dissociation model and color change mechanism of PDA/ZnO nanocomposites at low and high pH. Reproduced from ref. 61 with permission from Elsevier, copyright [2014].

turning purple (80 °C), red (100 °C) and yellow (100 °C), which is attributed to covalent interactions between PDA and silica in the films.

Combining PDA with metal oxides has been demonstrated to impact sensing properties with varied results. Attractive forces between PDA headgroups and surface charges on metal oxide nanoparticles stabilize the systems to thermal exposure and provide colorimetric reversibility on cooling. Similar stabilization is achieved upon exposure to organic solvents which allows PDA to be immobilized in a range of new polymers. The dissociation of metal oxides at low pH provides new colorimetric sensitivity in the acidic pH range. The increased thermal and chemical resistance of PDA/metal oxide nanocomposites has the potential to increase sensor specificity if they could be combined with surface conjugated recognition elements. Further work is required to investigate this potential.

Alterations to polydiacetylene format

PDA format refers to the size and morphology of the nanoparticles and the media on/in which PDA is fabricated, which can all impact sensor performance. Starting with the nano-

particles structure, Jia *et al.* demonstrated a 16 times higher sensitivity (detection limit of ~5 μM) for H_2O_2 detection when PDA sensors are functionalized with phenylboronic acid (PBA).[32] The addition of PBA alters the PDA vesicles shape from large spherical to small rod-shaped and square particles, which then improved detection sensitivity and stabilities by providing higher surface binding sites.

The advantage of PDA in film format was evident in the PDA-polydimethylsiloxane (PDMS) composite film sensor by Park *et al.*[67] Here, the mechanochromism properties of PDA were explored. The mechanical strain on PDA for colorimetric transition was induced by the swelling of PDMS elastomer in response to the exposure of saturated aliphatic hydrocarbons (SAHCs). The resulting flexible, transparent and 600 μm thick PDA-PDMS film is depicted in Fig. 19a and the incorporation of PDA vesicles dispersed in the PDMS matrix is shown in the optical microscopic image Fig. 19b. When incubated in pentane (C5), the PDA-PDMS film grew in concert with the gradual color change from blue to purple (Fig. 19c), before becoming a permanent red. Furthermore, whilst color change was irreversible, the opposite was true on the size change as the film shrunk to its original volume upon removal from SAHC solution.

The PDA-PDMS film swelling ratio and time for color change were found to be dependent of the aliphatic hydrocarbon chain length. These attributes are advantageous particularly for fake petroleum detection, as it enables simple colorimetric differentiation between various C5–C14 aliphatic hydrocarbons. Experimental data showed that after 10 min of SAHC incubation, the degree of swelling and red intensity decreased with longer chain length (Fig. 19d). As reasonably expected, the time for PDA-PDMS film to reach a fixed red intensity (75% RI) after SAHC exposure was longer with larger number of carbons (Fig. 19e). This difference was due to the variable extent and position of PDA crystals rupture when exposed to particular SAHC.

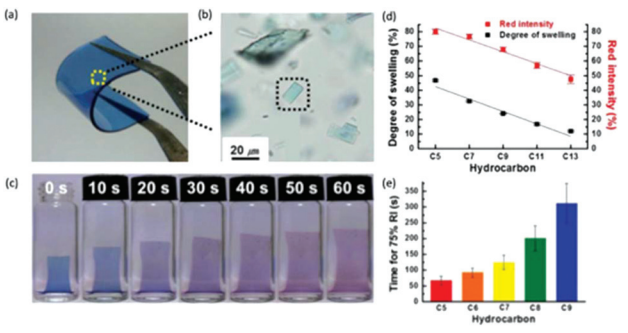

Fig. 19 (a) Photograph of PDA-embedded PDMS film. (b) Optical microscopic image of dispersed PDA vesicles in the PDMS matrix. (c) Time dependent colorimetric response and swelling of PDA-PDMS film incubated in pentane solvent. (d) Relationship between degree of swelling, red intensity and hydrocarbon chain length after 10 minutes incubation in saturated aliphatic hydrocarbons. (e) Time required for film to reach 75% of red intensity (RI). Reproduced from ref. 67 with permission from WILEY-VCH Verlag GmbH & Co., copyright [2014].

The morphological modification of PDA to improve sensitivity was investigated on a 3D network system by Lee *et al.*[68] The authors recognized the intrinsic sensitivity limitations when PDA is in 2D chip format (Fig. 20a) and fabricated a 3D networked PDA sensor system (Fig. 20b) for the detection of cyclodextrins (CDs). Briefly, micropillar structures made of p-type silicon (100) substrate were designed using deep etching process (Fig. 20c and d). Carbon nanotubes (CNTs) network were fabricated on the pillar structure to improve the immobilization of PDA vesicles (Fig. 20e), and Al_2O_3 coating was applied on the CNT network using atomic layer deposition method to enhance the mechanical integrity and introduce amine functional groups (Fig. 20f).

The 3D PDA network was exposed to α-CD solutions of various concentrations and the fluorescence intensity was compared to 2D PDA chips sensor produced using amine modified silicon wafer under similar conditions to the 3D sensor. Fig. 20g shows that the fluorescence intensity of 2D PDA chip began to increase only after 2.5 mM of CD, whereas the 3D network system displayed a gradual increase from micromolar to millimolar concentration. A significant increase

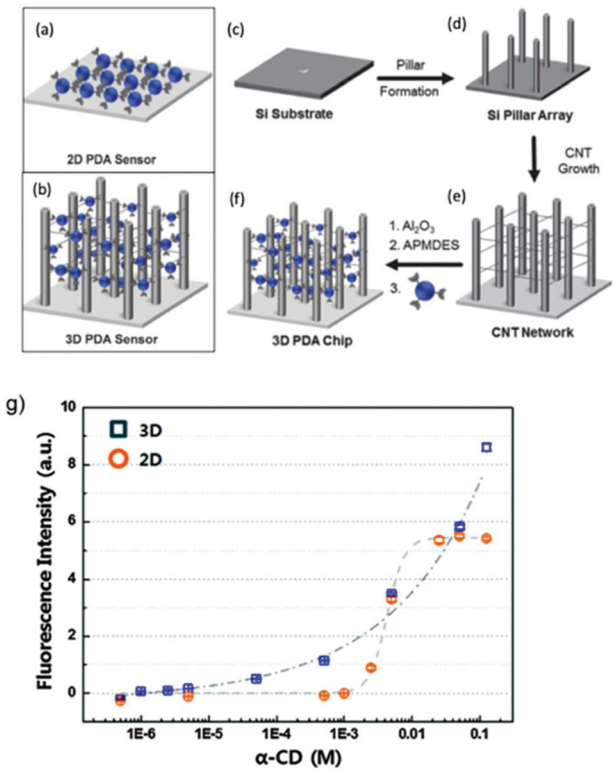

Fig. 20 Schematic diagram of (a) 2D PDA sensor, (b) 3D PDA network system, and the fabrication steps of the 3D PDA network system. Silicon substrate (c) is used to build micropillar arrays (d), which are then used to fabricate CNT network (e) where PDA vesicles are immobilized to form the final 3D PDA sensor network system (f). (g) Comparison of fluorescence intensity between the 2D and 3D PDA sensor when exposed to various concentration of cyclodextrin (α-CD). Reproduced from ref. 68 with permission from the Royal Society of Chemistry, copyright [2016].

of sensitivity was achieved due to the increased accessibility of CD molecules to interact with the higher number of exposed PDA vesicles in the 3D sensor matrix. In contrast, higher concentration of CD was required in 2D chips due to the aggregated nature of the PDA vesicles, which significantly prevented the CD–PDA interaction. The 3D network system improved the detection limit by at least three order, from 2.5 mM (2D chip) to 2.0 μM (3D network).

PDA can also be molded into solid substrates to alter its physical form to suit its application. For example, Chae *et al.* fabricated a directly writable thermochromic PDA-wax composites sensor using a simple mixing-molding method (Fig. 21a).[69] Hot solution comprised of 98% paraffin wax and 2% PDA was poured into a mold, cooled and removed. During the molding process, the wax molecules migrate into the single diacetylene (DA) crystal which induced crystal growth (Fig. 21b). When the UV polymerized PDA-wax composite (Fig. 21c) was subjected to heat, the monomers were released from the crystal, causing shrinkage (Fig. 21d) which then allowed the PDA C–C bond to rotate for the blue-red color change.

The reversibility properties can be adjusted as required. Chromic irreversibility can be attained with PCDA monomer (Fig. 22a), whereas reversibility can be achieved when using benzoic acid containing DA monomer 3-pentacosa-10,12-diynamidobenzoic acid (PCDA-mBzA) (Fig. 22b). Similarly, the transition temperature of the composite can be tuned by incorporating wax with different melting point. The experiment conducted by Chae *et al.*[69] reported that the color change was first observed at 70 °C and 90 °C for PCDA-wax composite and PCDA-mBzA wax, respectively.

Park *et al.* exploited the use of PDA as amphiphilic precursor that can be used on inkjet printers for hydrochromic imaging on paper.[70] The applications of this sensor include sweat-pore based identification systems employed in criminal

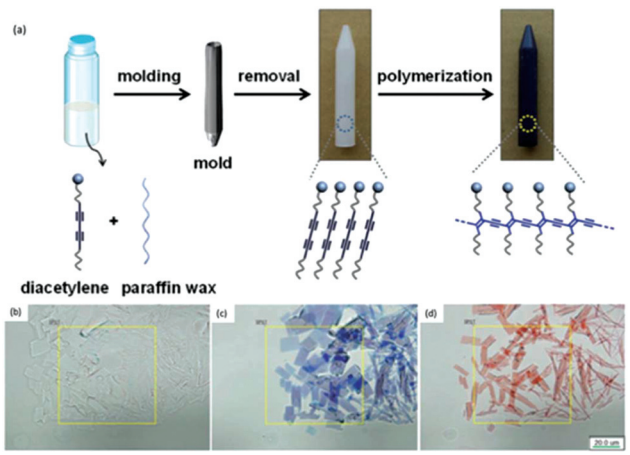

Fig. 21 (a) Schematic diagram of the PDA-paraffin wax composite sensor synthesis. Optical microscopic images of PDA-wax composite (b) before 254 nm UV irradiation, (c) after irradiation, and (d) after heat treatment at 55 °C for 10 seconds. Scale bars are 20 μm. Reproduced from ref. 69 with permission from WILEY-VCH Verlag GmbH & Co., copyright [2016].

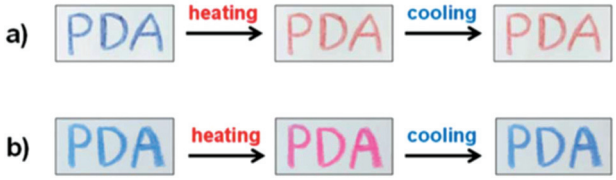

Fig. 22 Handwritten PDA image on paper derived from (a) PDA-wax when heated at 70 °C for 30 seconds then cooled and (b) colorimetric response of PDA-mBzA-wax heated to 120 °C and cooled. Reproduced from ref. 69 with permission from WILEY-VCH Verlag GmbH & Co., copyright [2016].

investigations, license validations and biometric security. The group was able to fabricate a PDA system that is stable under high relative humidity (>90%) and is printable on conventional paper. The printing ink was made with deionized water solution of imidazolium containing PCDA monomer, then diluted with 20% volume of ethanol. Upon UV irradiation, blue colored images were formed and red color was developed when in contact with water (Fig. 23a). It was also demonstrated that the intensity of the blue to red color transition was dependent on the water quantity used to overcoat the PDA printed regions on the paper (Fig. 23b). Furthermore, the chromatic transition sensitivity appeared to not be affected when conventional printer ink was overlayed on the PDA-printed region (Fig. 23b, middle). It was also shown that the colorimetric transition upon water contact was temperature dependent and only occurred above 20 °C (Fig. 23c). The image was stable for >1 month when stored at ambient condition and over 6 months in the refrigerator.

In addition to examples highlighted above, the embedding of polydiacetylenes in matrices, such as polymer hydrogels,[71–73] polymer fibers,[74–77] and polymer thin films,[21,78] have been reported with the aim to overcome aggregation of PDA vesicles, to influence the polymerization behavior of DA monomers, and/or to enhance the sensitivity of PDA sensors. PDA-embedded polymer matrices can be fabricated using various techniques, including electrospinning,[74–77] spin-coating,[79–82] and drop-casting.[78,83]

Tu *et al.* incorporated 10,12-docosadiynoic acid into matrix polymers made of PVP, polyethylene glycol, polyacrylic acid, or poly-4-vinylpyridine.[84] The PDA/matrix polymers enabled discrimination between VOCs (dichloromethane, chloroform, tetrahydrofuran, ethanol, and toluene) after exposure at 0.4% (v/v) for 5 minutes, owing to the solubility and chemical affinity of the matrix polymers with VOCs. The ratio of PDA to polymer was optimized to maximize the chromatic transition for a constant VOC concentration using RGB analysis with ImageJ freeware. The authors successfully demonstrated the ability to tune PDA sensitivity with specificity by embedding in an appropriate polymer matrix. Furthermore, the PDA/matrix polymer membranes could be stored at room temperature for up to 3 months without affecting the solvatochromic response.

Dolai *et al.* increased the sensitivity and specificity of PDA systems using a dual approach.[20] They synthesized a highly

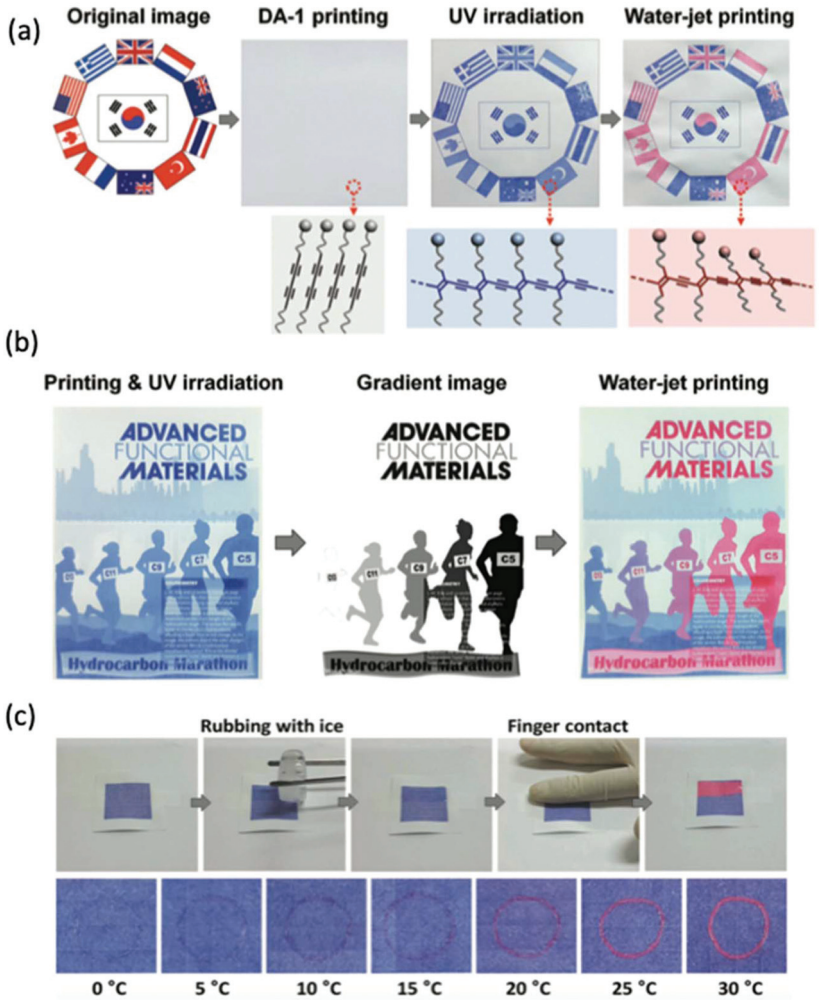

Fig. 23 (a) Inkjet printing of PDA sensor before and after UV irradiation, and after exposed with water. (b) A gradient color image showing the chromic transition is dependent on the water quantity. Color transition still occurred when overlayed with conventional ink cartridge. (c) Temperature-dependent colorimetric response of PDA-coated paper. No color change occurred unless surface was warmed upon finger contact. Reproduced from ref. 70 with permission from WILEY-VCH Verlag GmbH & Co., copyright [2016].

porous PDA-silica aerogel in which they drop-cast TRCDA monomers on aerogel powder, which then could be polymerized to form blue-phase PDA. The high porosity of the aerogel allowed rapid diffusion of VOC through the gel, which increased the reaction kinetics towards all fluids by enabling easier diffusion through the materials. To provide specificity, the head groups of the DA monomers were modified to discriminate between benzene, acetone, toluene, 2-propanol, pentane and diethyl ether (exposure at 1000 ppm for 60 minutes). In a similar dual approach, PDA/PVP was spin-coated to generate a uniform thin film on electrodes.[85] Upon physical or chemical absorption of VOCs, the dielectric properties of the PDA/PVP medium changed, enabling their application as capacitive sensors. The head groups of PDAs were altered to control selective absorption and discrimination between DMF, ethanol, *n*-propanol, iso-propanol, *n*-butanol, *n*-pentanol and acetone at 300 ppm. The authors reported that the chromatic sensitivity of the system could also be increased non-specifically by increasing the degree of photopolymerization.

Electrospun fibers have attracted great attention as a method of formatting PDA to increase sensitivity. Electrospinning technique involves applying a high voltage to a conductive capillary attached to a reservoir containing a polymer solution.[86–88] A charged polymer jet continuously ejects from the surface of the polymer solution when the charge imbalance exceeds the surface tension of the polymer solution, leading to the formation of thin non-woven fibers on a collector. This is a rapid and cost-effective technique for producing micro- and nanofibers with an enhanced surface area and porosity for the development of highly sensitivity detection systems. Chae *et al.* synthesized electrospun fibers from poly(ethylene oxide) (PEO) and PCDA, and DA monomers self-assembled during fiber formation.[74] Using scanning electron microscopy imaging, they showed fibers with highly uniformed diameters of 3 μm, providing a high surface area to

volume ratio. The PDA/polymer fiber sensors were used to distinguish α-CD to β- and γ-CD. Peng *et al.* achieved the first current-induced blue-to-red color transition in PDA by electrospinning electrochromatic carbon nanotube/PDA nanocomposite fibers.[75] The fibers rapidly and reversibly provide a visible blue-to-red response to changes in electrical current. More recently, Jeon *et al.* synthesized DA monomers containing a trimethyl amine (PCDA-DMEDA) and incorporated them with PEO into electrospun fibers and thin films to detect HCl gas.[76] Only the DA-electrospun fibers could be successfully photopolymerized to form blue-phase PDA. The results of both Peng[75] and Jeon[76] indicate that electrospinning of PDA into microfibers not only provides a high surface area to volume ratio but also allows favorable arrangement for DA photopolymerization into PDA. Yapor *et al.* synthesized electrospun fibers from PDA–PEO and PDA-polyurethane (PDA-PU) to detect *Escherichia coli*.[77] It was demonstrated that controlling the ratio of PEO and PU to PDA tuned the morphology and surface area of the fibers, which impacted the colorimetric response to bacterial supernatants.

Overall, studies have shown that alterations to PDA format could increase the performance of PDA-based sensors by improving the detection sensitivity, enhancing the structural integrity and stability by increasing the amount and accessibility of surface binding sites. In addition to improving the selectivity of PDA-based sensors, the easy customization of the end-products' physical form to better suit their application would mean that there is a greater chance of translating PDA sensors research into applicable technology. Further studies on the format alteration should be done to fully exploit the potential of PDA sensors for real-world applications.

Conclusions

To conclude, the discussed methods for tuning PDA performance can all be used to adjust sensitivity to detect analytes in the desired concentration region. However, some methods provide non-specificity, *i.e.* creating a corresponding undesired increase in sensitivity towards environmental stimulus. Adjusting the alkyl chain length, increasing photopolymerization time, and lipid doping all increase PDA sensitivity towards light, temperature and the chemical environment. Other methods, including metal and non-metal oxide doping, head group modification, and PDA formatting typically stabilize PDA in the face of environmental stimulus and can be engineered to increase sensitivity towards the desired analyte with specificity. This review also emphasizes the tunable chromic reversibility of PDA sensors, which was proven advantageous due to its customizable real-time applications.

Although various highly sensitive, stable, and specific PDA-based probes for many applications have been developed, challenges still remain. For more practical applications as sensing platform, further research should focus on addressing the susceptibility with environmental stimuli by reverse engineering the PDA-based sensors materials and format. For example, it may be possible that the changes due to undesired stimuli be used to trigger the activation of alternative molecule which ultimately improves the overall sensitivity, stability and selectivity. Modifying the receptor moiety by doping with stimuli-responsive block copolymers or nanoengineered templated PDA particles could be explored.

This review also highlights the importance of determining the point of balance when improving one performance characteristic does not compromise the integrity of another, such as the counteracting effect found between the head groups and the structural intermolecular forces in some compounds. As the performance of PDA sensors are dependent of many chemical and physical parameters, rigorous theoretical studies and simulations of this material is required to better comprehend its behavior. This necessitates the needs for more research and collaborative efforts from various disciplines to design techniques that can tune sensor performance to enable high sensitivity in the face of environmental stimulus. More specifically, as PDA-nanosensors physical form can be altered to suit its application, future work should not only focus on understanding the fundamental chemistry and improving performance, but also on selecting the most suitable format that can ultimately be used in various real-time products. Achieving this will allow better translation of the academic research on PDA sensors into applicable technology.

Conflicts of interest

There are no conflicts to declare.

Acknowledgements

M. W. acknowledges the support from the Australian Government Research Training Program Scholarship. R. C. acknowledges the support from the Australian Research Council Discovery Early Career Researcher Award (ARC DECRA DE170100068) and the UNSW Scientia Fellowship.

Notes and references

1 J. Deschamps, M. Balog, B. Boury, M. Ben Yahia, J.-S. Filhol, A. van der Lee, A. Al Choueiry, T. Barisien, L. Legrand, M. Schott and S. G. Dutremez, *Chem. Mater.*, 2010, **22**, 3961.
2 D.-Y. Kim, S.-A. Lee, D. Jung, J. Koo, J. S. Kim, Y.-T. Yu, C.-R. Lee and K.-U. Jeong, *Soft Matter*, 2017, **13**, 5759.
3 M. J. Kim, S. Angupillai, K. Min, M. Ramalingam and Y.-A. Son, *ACS Appl. Mater. Interfaces*, 2018, **10**, 24767.
4 D. Krishnan, A. Raj R B and E. B. Gowd, *Polym. Chem.*, 2019, **10**, 3154.
5 Y. Scindia, L. Silbert, R. Volinsky, S. Kolusheva and R. Jelinek, *Langmuir*, 2007, **23**, 4682.

6 J. Park, S. K. Ku, D. Seo, K. Hur, H. Jeon, D. Shvartsman, H.-K. Seok, D. J. Mooney and K. Lee, *Chem. Commun.*, 2016, **52**, 10346.
7 E. Lebègue, C. Farre, C. Jose, J. Saulnier, F. Lagarde, Y. Chevalier, C. Chaix and N. Jaffrezic-Renault, *Sensors*, 2018, **18**, 599.
8 S. Seo, J. Lee, E.-J. Choi, E.-J. Kim, J.-Y. Song and J. Kim, *Macromol. Rapid Commun.*, 2013, **34**, 743.
9 L. Jiang, J. Luo, W. Dong, C. Wang, W. Jin, Y. Xia, H. Wang, H. Ding, L. Jiang and H. He, *J. Virol. Methods*, 2015, **219**, 38.
10 Y. K. Jung, T. W. Kim, H. G. Park and H. T. Soh, *Adv. Funct. Mater.*, 2010, **20**, 3092.
11 J. d. P. Rezende, G. M. D. Ferreira, G. M. D. Ferreira, L. H. M. da Silva, M. do Carmo Hepanhol da Silva, M. S. Pinto and A. C. d. S. Pires, *Mater. Sci. Eng., C*, 2017, **70**, 535.
12 Y. K. Jung and H. G. Park, *Sens. Actuators, B*, 2019, **278**, 190.
13 D. H. Kang, H.-S. Jung, N. Ahn, J. Lee, S. Seo, K.-Y. Suh, J. Kim and K. Kim, *Chem. Commun.*, 2012, **48**, 5313.
14 G. Zhou, F. Wang, H. Wang, S. Kambam and X. Chen, *Macromol. Rapid Commun.*, 2013, **34**, 944.
15 X. Chen, S. Kang, M. J. Kim, J. Kim, Y. S. Kim, H. Kim, B. Chi, S.-J. Kim, J. Y. Lee and J. Yoon, *Angew. Chem., Int. Ed.*, 2010, **49**, 1422.
16 K. M. Lee, J. H. Moon, H. Jeon, X. Chen, H. J. Kim, S. Kim, S.-J. Kim, J. Y. Lee and J. Yoon, *J. Mater. Chem.*, 2011, **21**, 17160.
17 J. Guo, L. Yang, L. Zhu and D. Chen, *Polymer*, 2013, **54**, 743.
18 D. H. Kang, H.-S. Jung, N. Ahn, S. M. Yang, S. Seo, K.-Y. Suh, P.-S. Chang, N. L. Jeon, J. Kim and K. Kim, *ACS Appl. Mater. Interfaces*, 2014, **6**, 10631.
19 D.-H. Park, J.-M. Heo, W. Jeong, Y. H. Yoo, B. J. Park and J.-M. Kim, *ACS Appl. Mater. Interfaces*, 2018, **10**, 5014.
20 S. Dolai, S. K. Bhunia, S. S. Beglaryan, S. Kolusheva, L. Zeiri and R. Jelinek, *ACS Appl. Mater. Interfaces*, 2017, **9**, 2891.
21 L. H. Nguyen, S. Naficy, R. McConchie, F. Dehghani and R. Chandrawati, *J. Mater. Chem. C*, 2019, **7**, 1919.
22 F. Mazur, M. Bally, B. Städler and R. Chandrawati, *Adv. Colloid Interface Sci.*, 2017, **249**, 88.
23 Y.-R. Kim, S. Jung, H. Ryu, Y.-E. Yoo, S. M. Kim and T.-J. Jeon, *Sensors*, 2012, **12**, 9530.
24 G. Wegner, *Z. Naturforsch., B: J. Chem. Sci.*, 1969, **24**, 824.
25 X. Q. Chen, G. D. Zhou, X. J. Peng and J. Yoon, *Chem. Soc. Rev.*, 2012, **41**, 4610.
26 R. Jelinek and M. Ritenberg, *RSC Adv.*, 2013, **3**, 21192.
27 J. T. Wen, J. M. Roper and H. Tsutsui, *Ind. Eng. Chem. Res.*, 2018, **57**, 9037.
28 X. M. Qian and B. Städler, *Chem. Mater.*, 2019, **31**, 1196.
29 N. Traiphol, K. Faisadcha, R. Potai and R. Traiphol, *J. Colloid Interface Sci.*, 2015, **439**, 105.
30 S. Okada, S. Peng, W. Spevak and D. Charych, *Acc. Chem. Res.*, 1998, **31**, 229.
31 D. H. Kang, H. S. Jung, J. Lee, S. Seo, J. Kim, K. Kim and K. Y. Suh, *Langmuir*, 2012, **28**, 7551.
32 C. Jia, J. Tang, S. Lu, Y. Han and H. Huang, *J. Fluoresc.*, 2016, **26**, 121.
33 H. U. Lee, H. Kim, K.-Y. Chun, C. H. Kwon, M. D. Lima, R. H. Baughman and S. J. Kim, *Smart Mater. Struct.*, 2016, **25**, 075021.
34 D. Charych, Q. Cheng, A. Reichert, G. Kuziemko, M. Stroh, J. O. Nagy, W. Spevak and R. C. Stevens, *Chem. Biol.*, 1996, **3**, 113.
35 N. Charoenthai, T. Pattanatornchai, S. Wacharasindhu, M. Sukwattanasinitt and R. Traiphol, *J. Colloid Interface Sci.*, 2011, **360**, 565.
36 A. Chanakul, N. Traiphol and R. Traiphol, *J. Colloid Interface Sci.*, 2013, **389**, 106.
37 J.-M. Kim, J.-S. Lee, H. Choi, D. Sohn and D. J. Ahn, *Macromolecules*, 2005, **38**, 9366.
38 S. Wu, F. Shi, Q. Zhang and C. Bubeck, *Macromolecules*, 2009, **42**, 4110.
39 H. Jiang, Y. Wang, Q. Ye, G. Zou, W. Su and Q. Zhang, *Sens. Actuators, B*, 2010, **143**, 789.
40 A. Kamphan, C. Khanantong, N. Traiphol and R. Traiphol, *J. Ind. Eng. Chem.*, 2017, **46**, 130.
41 C. Khanantong, N. Charoenthai, T. Phuangkaew, F. Kielar, N. Traiphol and R. Traiphol, *Colloids Surf., A*, 2018, **553**, 337.
42 U. Jonas, K. Shah, S. Norvez and D. H. Charych, *J. Am. Chem. Soc.*, 1999, **121**, 4580.
43 D.-H. Park, B. J. Park and J.-M. Kim, *Macromol. Res.*, 2016, **24**, 943.
44 S. Toommee, R. Traiphol and N. Traiphol, *Colloids Surf., A*, 2015, **468**, 252.
45 A. Kamphan, N. Traiphol and R. Traiphol, *Colloids Surf., A*, 2016, **497**, 370.
46 O. Mapazi, P. K. Matabola, R. M. Moutloali and C. J. Ngila, *Sens. Actuators, B*, 2017, **252**, 671.
47 I. S. Park, H. J. Park, W. Jeong, J. Nam, Y. Kang, K. Shin, H. Chung and J.-M. Kim, *Macromolecules*, 2016, **49**, 1270.
48 M. Wang, F. Wang, Y. Wang, W. Zhang and X. Chen, *Dyes Pigm.*, 2015, **120**, 307.
49 M. Cox and D. Nelson, *Lehninger Principles of Biochemistry*, 2000.
50 F. C. O. Los, T. M. Randis, R. V. Aroian and A. J. Ratner, *Microbiol. Mol. Biol. Rev.*, 2013, **77**, 173.
51 G. Valincius and R. Budvytyte, *Phospholipid Sensors for Detection of Bacterial Pore-Forming Toxins*, 2014.
52 D. H. Kang, H.-S. Jung, J. Lee, S. Seo, J. Kim, K. Kim and K.-Y. Suh, *Langmuir*, 2012, **28**, 7551.
53 S.-i. M. Nomura, Y. Mizutani, K. Kurita, A. Watanabe and K. Akiyoshi, *Biochim. Biophys. Acta, Biomembr.*, 2005, **1669**, 164.
54 C. X. Guo, P. Boullanger, T. Liu and L. Jiang, *J. Phys. Chem. B*, 2005, **109**, 18765.
55 G. Kim, S. Song, J. Lee and J.-M. Kim, *Langmuir*, 2010, **26**, 17840.

56 K.-W. Kim, H. Choi, G. S. Lee, D. J. Ahn and M.-K. Oh, *Colloids Surf., B*, 2008, **66**, 213.
57 A. Patlolla, J. Zunino, A. I. Frenkel and Z. Iqbal, *J. Mater. Chem.*, 2012, **22**, 7028.
58 A. Wu, C. Beck, Y. Ying, J. Federici and Z. Iqbal, *J. Phys. Chem. C*, 2013, **117**, 19593.
59 A. Wu, Y. Gu, C. Beck, Z. Iqbal and J. F. Federici, *Sens. Actuators, B*, 2014, **193**, 10.
60 A. Wu, Y. Gu, C. Stavrou, H. Kazerani, J. F. Federici and Z. Iqbal, *Sens. Actuators, B*, 2014, **203**, 320.
61 A. Chanakul, N. Traiphol, K. Faisadcha and R. Traiphol, *J. Colloid Interface Sci.*, 2014, **418**, 43.
62 A. Chanakul, R. Traiphol and N. Traiphol, *Colloids Surf., A*, 2016, **489**, 9.
63 S. Toommee, *Colloids Surf., A*, 2015, **468**, 252.
64 H. Peng, J. Tang, J. Pang, D. Chen, L. Yang, H. S. Ashbaugh, C. J. Brinker, Z. Yang and Y. Lu, *J. Am. Chem. Soc.*, 2005, **127**, 12782.
65 A. Nopwinyuwong, W. Boonsupthip, C. Pechyen and P. Suppakul, *Adv. Polym. Technol.*, 2013, **32**, E724.
66 H. Wang, S. Han, Y. Hu, Z. Qi and C. Hu, *Colloids Surf., A*, 2017, **517**, 84.
67 D.-H. Park, J. Hong, I. S. Park, C. W. Lee and J.-M. Kim, *Adv. Funct. Mater.*, 2014, **24**, 5186.
68 S. Lee, J. Lee, D. W. Lee, J. M. Kim and H. Lee, *Chem. Commun.*, 2016, **52**, 926.
69 S. Chae, J. P. Lee and J.-M. Kim, *Adv. Funct. Mater.*, 2016, **26**, 1769.
70 D.-H. Park, W. Jeong, M. Seo, B. J. Park and J.-M. Kim, *Adv. Funct. Mater.*, 2016, **26**, 498.
71 M. Gou, X. Qu, W. Zhu, M. Xiang, J. Yang, K. Zhang, Y. Wei and S. Chen, *Nat. Commun.*, 2014, **5**, 3774.
72 S. Seo, J. Lee, M. S. Kwon, D. Seo and J. Kim, *ACS Appl. Mater. Interfaces*, 2015, **7**, 20342.
73 Y. T. Kim, D. Ma, J. K. Sim and S.-H. Kim, *Ultrasound Med. Biol.*, 2018, **44**, 1799.
74 S. K. Chae, H. Park, J. Yoon, C. H. Lee, D. J. Ahn and J.-M. Kim, *Adv. Mater.*, 2007, **19**, 521.
75 H. Peng, X. Sun, F. Cai, X. Chen, Y. Zhu, G. Liao, D. Chen, Q. Li, Y. Lu, Y. Zhu and Q. Jia, *Nat. Nanotechnol.*, 2009, **4**, 738.
76 H. Jeon, J. Lee, M. Kim and J. Yoon, *Macromol. Rapid Commun.*, 2012, **33**, 972.
77 J. P. Yapor, A. Alharby, C. Gentry-Weeks, M. M. Reynolds, A. K. M. Mashud Alam and Y. V. Li, *ACS Omega*, 2017, **2**, 7334.
78 J. Lee, O. Yarimaga, C. H. Lee, Y.-K. Choi and J.-M. Kim, *Adv. Funct. Mater.*, 2011, **21**, 1032.
79 J. Lee, M. Pyo, S.-h. Lee, J. Kim, M. Ra, W.-Y. Kim, B. J. Park, C. W. Lee and J.-M. Kim, *Nat. Commun.*, 2014, **5**, 3736.
80 K. Parambath Kootery, H. Jiang, S. Kolusheva, T. P. Vinod, M. Ritenberg, L. Zeiri, R. Volinsky, D. Malferrari, P. Galletti, E. Tagliavini and R. Jelinek, *ACS Appl. Mater. Interfaces*, 2014, **6**, 8613.
81 B.-y. Lee, J. Kim, W. J. Kim and J. K. Kim, *J. Membr. Sci.*, 2018, **549**, 680.
82 A. Trachtenberg, O. Malka, K. P. Kootery, S. Beglaryan, D. Malferrari, P. Galletti, S. Prati, R. Mazzeo, E. Tagliavini and R. Jelinek, *New J. Chem.*, 2016, **40**, 9054.
83 W. Zhang, H. Xu, Y. Chen, S. Cheng and L.-J. Fan, *ACS Appl. Mater. Interfaces*, 2013, **5**, 4603.
84 M.-C. Tu, J. A. Cheema, U. H. Yildiz, A. Palaniappan and B. Liedberg, *J. Mater. Chem. C*, 2017, **5**, 1803.
85 V. K. Rao, N. L. Teradal and R. Jelinek, *ACS Appl. Mater. Interfaces*, 2019, **11**, 4470.
86 J. Xue, J. Xie, W. Liu and Y. Xia, *Acc. Chem. Res.*, 2017, **50**, 1976.
87 L. A. Mercante, V. P. Scagion, F. L. Migliorini, L. H. C. Mattoso and D. S. Correa, *TrAC, Trends Anal. Chem.*, 2017, **91**, 91.
88 R. Chandrawati, M. T. J. Olesen, T. C. C. Marini, G. Bisra, A. G. Guex, M. G. de Oliveira, A. N. Zelikin and M. M. Stevens, *Adv. Healthcare Mater.*, 2017, **6**, 1700385.